THE JOURNAL OF PHYSICAL CHEMISTRY B

Article

pubs.acs.org/JPCB

Supported Lipid Monolayer with Improved Nanomechanical Stability: Effect of Polymerization

Racha El Zein, Hervé Dallaporta, and Anne M. Charrier*

CNRS, UMR7325, 13288, Marseille, France, and Aix-Marseille University, CINaM, 13288, Marseille, France

ABSTRACT: We study the effect of polymerization on the nanomechanical stability of supported lipid monolayers consisting of 1,2-di-(10Z,12Z-tricosadiynoyl)-sn-glycero-3-phosphocholine by means of force mapping using an atomic force microscope. For both nonpolymerized and polymerized lipid monolayers, we investigate the break-through forces required to rupture the monolayers for a whole range of loading velocities. We show that the average break-through force exerted by the tip and required to penetrate the monolayer has a logarithmic dependence on the loading rate. Both Young moduli and intrinsic Gibbs energies have been determined for the nonpolymerized and polymerized lipid monolayers, and we show a drastic effect of polymerization on the nanomechanical stability of the monolayer with an increase by a factor of ∼100 for the young modulus and ∼3 for the intrinsic Gibbs activation energy.

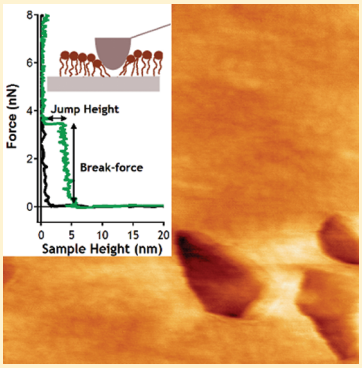

INTRODUCTION

Force measurement using atomic force microscopy (AFM) has now become a very common technique used to probe the nanomechanical properties of materials and especially those of thin films.[1−12] Among those, abundant studies realized on supported lipid bilayers[13−16] have shown that the variation of mechanical stability depends on the ordering of the lipids within the bilayer. The solid-like ordered phase with higher density of lipids shows higher mechanical stability than low density disordered phase.[17,18] That said, one knows that lipid bilayers exhibit gel to fluid phase transition in a range of temperatures that varies from −70 °C to +80 °C depending on their length, headgroup, and number of unsaturated bonds in their fatty acid chains. In addition, when these bilayers are supported, their interaction with the substrate may drastically increase their transition temperature.[19] It is therefore expected that the mechanical properties of lipid layers will strongly depend on the type of lipid constituting the layer and on the temperature at which the measurement is realized. Similarly it was shown that the composition of the lipid bilayer might vary considerably its mechanical stability.[20] For example, some recent studies show that increasing the ratio of cholesterol in a mixture of dioleoylphosphatidylcholine/sphongomyelin releases the stress in the layer and as a result lowers the breakthrough force required to induce rupture.[21] Understanding the mechanisms that govern the mechanics and elastic properties of lipid membranes is essential for both the comprehension of biological processes and the development of biotechnologies or bioinspired technologies. For example it was shown that elastic bilayer forces modulate the free energy and cooperativity of folding of membrane proteins[22] and transmembrane signaling.[23] Also, as a biocompatible material, some researchers have been working on the development of nanoparticles for the targeting and delivery of drugs in which lipid bilayers are used to encapsulate the drugs. In that field a lot of work is dedicated to controlling the stability of the bilayer.[24,25] Another example is the stabilization of supported lipid mono- and bilayers containing acryl and acetylenic species in air by polymerization therefore opening new opportunities of applications.[26] Typically, the electrical properties of polymerized lipid monolayers of tricosadiynoylphosphatidylcholine were recently reported[27] and suggested that such layers could be used as ultrathin dielectrics in electronic devices such as field effect transistors provided these present strong enough mechanical stability to handle advanced industrial processes.

In this work, we investigate the effect of polymerization on the nanomechanical stability of supported lipid monolayers. Force measurements using AFM were realized before and after polymerization on same supported lipid monolayers. In a typical force measurement, the AFM tip, initially far from the surface approaches the sample and gets into contact with the lipid monolayer. As the tip keeps moving toward the substrate, the cantilever, with a given spring constant, bends over the lipid layer until the exerted force becomes large enough to rupture the layer. At this point the tip jumps to the substrate and the jump height of the tip corresponds to the thickness of the layer under the compression of the tip. Both the break-through force and the jump height are parameters of the considered lipid layer that can be utilized to determine properties of the layer. In addition, indentation experiments on lipid bilayers have revealed that the rate of formation of a hole, large enough to initiate the tip penetration in the bilayer, is governed by an

Received: March 9, 2012
Revised: May 31, 2012
Published: June 1, 2012

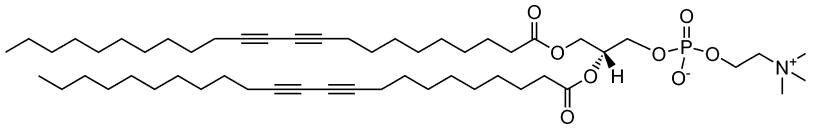

Figure 1. Scheme of 1,2-di-(10Z,12Z-tricosadiynoyl)-sn-glycero-3-phosphocholine, DC8,9PC, lipid.

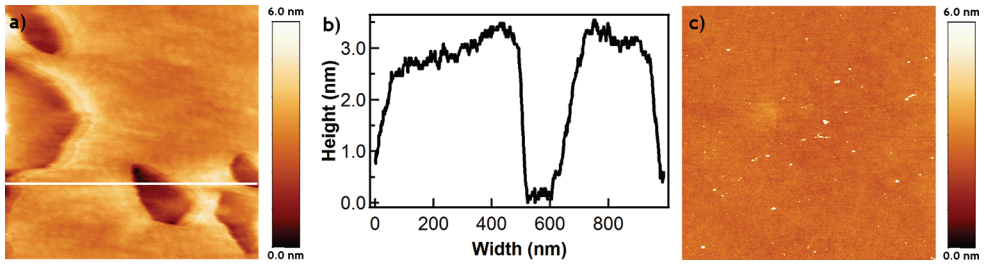

Figure 2. AFM images of (a) DC8,9PC monolayer with holes imaged in solution, 1 × 1 μm^2. The presence of the holes allows for the determination of the thickness of the monolayer. (b) Cross-section of the monolayer indicating a thickness of 3 ± 0.3 nm. (c) Homogeneous DC8,9PC monolayer with no holes or overlayers imaged in air, 5 × 5 μm^2.

activation energy following an Arrhenius law.[28−30] It was shown that this intrinsic Gibbs energy of a bilayer-tip system to spontaneously form a hole in the bilayer can be increased by the application of a pressure on the bilayer therefore favoring its rupture.[28] The rate at which the pressure increases being tip loading rate dependent, the Gibbs energy not only depends on the properties of the investigated bilayer but also on the tip loading rate used in the experiment. If this kind of behavior is well-known for lipid bilayers it was never demonstrated for monolayers. We investigate the effect of the loading rate on the monolayer rupture for both types of monolayers and we will show how the polymerization impacts the nanomechanical resistance of the monolayer. From the experimental data we determine the Young's modulus and the intrinsic Gibbs energy of each type of monolayer.

MATERIALS AND METHODS

Materials. The lipids, 1,2-di-(10Z,12Z-tricosadiynoyl)-sn-glycero-3-phosphocholine, DC8,9PC, (Figure 1) were purchased from Avanti Polar Lipids (Alabster, AL) and used without further purification. A 1 mg/mL lipid stock solution was prepared in chloroform and stored at −20 °C. These lipids were selected for having two acetylenic groups in each of their aliphatic chains, therefore allowing for two-dimensional polymerization in the plane of the layer. Polymerization initiator (2,2-azobis(2-methylpropionamidine)dihydrochloride (AAPH), methanol, chloroform, sulphuric acid, 96% (H_2SO_4), hydrofluoric acid, 49% (HF) and hydrogen peroxide, and 30% (H_2O_2) were purchased from Sigma Aldrich. Deionized water (DI, 18 MΩ·cm) was used in all experiments.

Silicon Surface Preparation. Silicon wafers ((100), ρ∼5 Ω.cm, Boron doped) were cleaned by soaking in 2:1 H_2SO_4/H_2O_2 (piranha solution) at 130 °C for 30 min, followed by thorough rinsing with DI water. Just prior to forming the lipid monolayer, H-terminated silicon surface is obtained by etching off the native silicon oxide from the silicon substrate with HF (2 min in 2% ethanol). The hydrogen passivation results from efficient removal of fluorine-bonded surface silicon as SiF_4 leaving behind hydrogen.[31]

Vesicles Preparations. A total of 50 μL of the 0.1% lipid stock solution were heated at 40 °C to evaporate chloroform and then diluted in 200 μL of DI water. At this stage multilamellar lipid vesicles are formed in the aqueous solution. Unilamellar vesicles are then obtained by sonication of the lipid solution for 15 min. Finally the vesicle radius was reduced by extrusion through 100 nm pores polycarbonate membrane.

Monolayer Preparation and Polymerization. We have developed a method to form a dense and homogeneous lipid monolayer directly at the surface of silicon (after etching off the SiO_2). This method is based on the vesicle fusion technique, commonly used to fabricate supported bilayers on hydrophilic substrates. In the case of hydrophobic surfaces the fusion of vesicles is not simple, the interaction between the hydrophilic headgroups of the lipids pointing toward the outside of the vesicles and a hydrophobic surface being energetically unfavorable. After formation of a H-terminated silicon surface, a concentrated solution of vesicles is deposited on the surface which is quickly cooled down to 10 °C. The formation of a dense and homogeneous layer is quasi-instantaneous. The sample is then slowly heated to 35 °C and rinsed with water. The monolayer is then stabilized in air by two-dimensional polymerization. AAPH (0.1%) free radical is added to the solution at 30 °C, and the sample is slowly heated (1 °C/min) to 40 °C at which the temperature is maintained for 15 min. During the overall experiment, the temperature is always maintained below the melting temperature of the lipids (43 °C); that is, the monolayer always is in its solid state. The sample is then slowly cooled to room temperature and rinsed with DI water. A very convenient way to verify the polymerization of the lipid monolayer has worked consists in rinsing the sample with methanol. When the lipids are not polymerized, this rinsing induces a complete wash off of the lipid monolayer, whereas it remains unchanged when polymerized. The thickness of dried as prepared monolayers measured by ellipsometry was previously reported and an average thickness of 2.7 ± 0.3 nm was measured.[27] Figure 2a shows an AFM image of a lipid monolayer that was measured in solution. Although this type of sample is not suitable for our study which requires a good homogeneity of the monolayer, the presence of holes offers the possibility to measure the thickness of the layer. Figure 2b shows a cross-section of the image and the depth of the hole can be estimated to 3 ± 0.3 nm. This thickness is in good agreement with measurements that were previously realized on lipid bilayers of DC8,9PC for which thicknesses of 6.6 nm were reported.[32] The difference between the ellipsometry and the AFM measurements may come from

dx.doi.org/10.1021/jp302306r | J. Phys. Chem. B 2012, 116, 7190−7195

the hydration of the layer that may change the molecules organization. Figure 2c shows an AFM image of a perfectly homogeneous monolayer with no holes or overlayers. Such monolayer quality is obtained on a regular base and was verified before any further measurements.

AFM Force Measurements. Force measurements were carried out in deionized water using AFM (NTEGRA from NT-MDT). Silicon tips CSC17 from MikroMash with a typical resonance frequency of 14 kHz in solution and tip radius in the range 8−10 nm were selected for this testing. The AFM tip radii were determined after imaging the tip by scanning electron microscopy. The spring constants in the range from 0.1 to 0.3 N/m were determined using the thermal noise method after obtaining the deflection sensitivity of the cantilever by pressing the AFM tip against a hard reference silicon surface. Cantilever deflection sensitivity measurements were performed before all sets of measurements. A minimum of 200 force measurements per set were realized on a minimum of three different areas per sample. To prevent any questioning regarding the reproducibility of the lipid monolayers quality and a misinterpretation of the data, all of the measurements reported as before and after polymerization were realized as pairs on the same sample using the same AFM tip.

RESULTS AND DISCUSSION

Dependence of the Break-through Force on the Polymerization State. Figure 3a shows two different representative force curves (loading part only) obtained on a hard silicon surface (black) and a lipid monolayer (green). From this type of measurement, one can determine the force required to rupture the monolayer as well as the height of the monolayer. The later is the sum of the indentation of the tip in the monolayer before the break-through occurs and the tip jump height at the break-through. Since a higher break-through force indicates a more resistant layer, both these parameters can be used to evaluate the nanomechanical stability of the lipid monolayers. To evaluate the effect of the polymerization, a statistical analysis of these break-through forces and tip jumps heights at the lipid monolayers rupture were realized before and after polymerization. In Figure 3b the break-through force versus the tip jump height is reported for over 400 measurements acquired before and after polymerization of the monolayers on three different samples and for a tip loading rate of 6 μm/s. The difference between the two types of lipid monolayers is evidenced in this figure. As an average force of 98 ± 67 pN is required to rupture the layer before polymerization, a net increase to 1.4 ± 0.72 nN is measured after polymerization. Although the large error bars which seem to indicate variability in the quality of the investigated lipid monolayers, the data clearly reveal an improvement of the nanomechanical resistivity of the monolayers after polymerization.

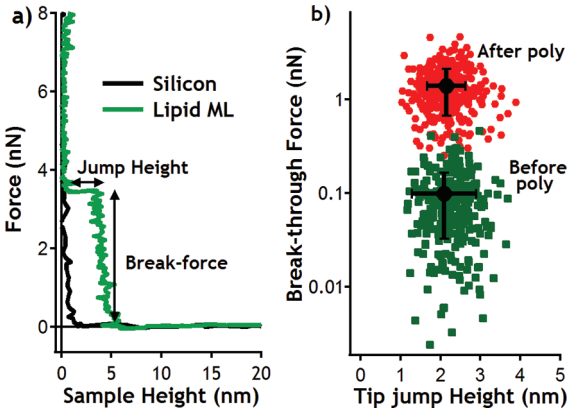

Figure 3. (a) Representative force measurements loading curves obtained on a hard silicon surface (black) and a supported lipid monolayer after polymerization (green). (b) Break-through forces versus the tip jumpin distance at the lipid monolayer rupture reported for over 400 measurements on three different samples before (green) and after (red) polymerization. The tip loading rate was 6 μm/s.

Dependence of the Break-through Force on the Loading Rate. Indentation experiments on lipid bilayers have shown that the average break-through force is logarithmically dependent on the loading rate at which the indentation is performed, i.e., on the rate at which the tip hits the lipid bilayer.[22,28−30] Although this property has now been well demonstrated for lipid bilayers it was never shown for monolayers. We present a statistical analysis of the force at which the break-through occurs for a whole range of loading rates varying from 30 nm·s^{-1} to 6 μm·s^{-1}. Because each monolayer is not perfectly identical, some differences appear between sets of measurements. For clarity, we will show the results obtained on one representative sample. In the following the sets of measurements were performed on the same monolayer before and after polymerization. These are shown in green square and red circle respectively. For each loading rate v, the average value F_0 is reported in Figure 4, each point corresponding to a sample of at least 200 force curve measurements. The first observation is that for both types of monolayer the average break-through force increases linearly with the logarithm of the loading rate similarly to what was reported for bilayers. The red and green lines result from fitting equation $F_0 = a + b \log(v)$ to the experimental data. The second observation is that the dependence of F_0 on the loading velocity is very different whether the lipid monolayer is polymerized. Before the polymerization, the break-through forces are very small with values ranging from 20 to 60 pN while still showing some dependence on the loading rate. To remove the tip curvature effect and compare these results with measurements obtained with different tips and samples we normalized these forces by the tip curvature.[16] We obtain normalized forces ranging from 2 to 7 mN·m^{-1}. Such values of

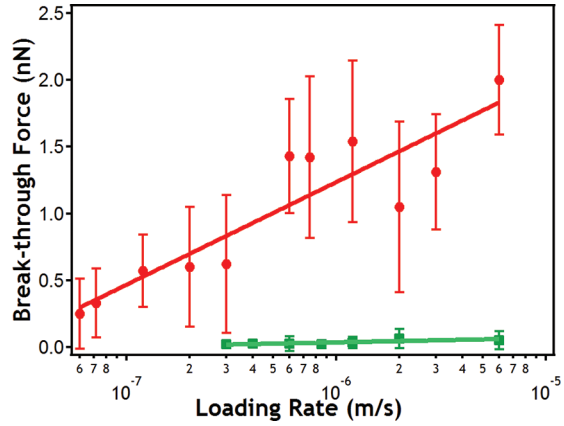

Figure 4. Average break-through forces obtained at loading rates ranging from 30 nm·s^{-1} to 6 μm·s^{-1} on both nonpolymerized (green squares) and polymerized (red circles) lipid monolayers.

dx.doi.org/10.1021/jp302306r | J. Phys. Chem. B 2012, 116, 7190−7195

the break-through forces are relatively small compared to those usually reported for bilayers (105 mN·m^{-1} for DSPE,[16] 220 mN·m^{-1} for MGDG,[16] 66−170 mN·m^{-1} for DOTAP,[27] 30 mN·m^{-1} for POPE/POPG mixtures,[33] 900 mN·m^{-1} for DMPC,[34] and 72 mN·m^{-1} for POPG[35]) but fall into the same range of values as previously reported for monolayers of DPPC[36] (DPPC and DC8,9PC have similar melting temperatures and headgroups. They are therefore expected to behave similarly). After polymerization the break-through forces are much bigger and vary between 0.2 and 2 nN for the investigated range of loading rates, therefore corresponding to normalized forces varying from 24 to 235 mN·m^{-1}. These values which compare with those obtained on bilayers evidence the impact of the polymerization on the nanomechanical resistance of the monolayer.

Determination of the Young's Modulus: Impact of the Polymerization. To determine the Young's modulus of each type of monolayer, we describe our experimental data in the framework of the Hertz model of a tip lipid monolayer system approximated by a sphere in contact with a flat surface. Using the radius of the contact area between the tip and the lipid monolayer $a = (Rh)^{1/2}$ and the indentation $h = h_0 - d_j$ at the rupture, one can relate the average break-through force to the tip jump height as

$$F_0 = \frac{4}{3}\frac{E}{(1-\nu^2)}\sqrt{R}(h_0 - d_j)^{3/2} \quad (1)$$

ν is the Poisson coefficient (we have used $\nu = 0.3$), E is the Young's modulus of the monolayer, R is the radius of the tip, h_0 is the thickness of the monolayer, and d_j is the jump height at the break-through.

Like for the break-through force we have determined for every loading rate the average tip jump height for both monolayers. The results are presented in the inset in Figure 5

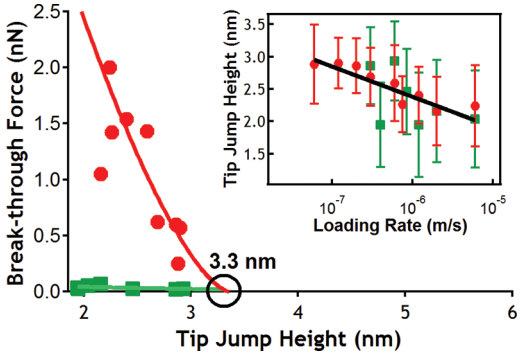

Figure 5. Average break-through forces versus average tip jumps-in obtained on nonpolymerized (green) and polymerized (red) lipid monolayers for loading rates in the range 60 nm·s^{-1} to 6 μm·s^{-1}. When the breakthrough force is zero, the tip jump corresponds to the thickness of the layer. Inset: Corresponding average tip jumps-in obtained at different loading rates.

and show that the jump height generally decreases, i.e., the indentation increases, with the loading rate (The black line is just a guide to the eye). This result is reasonable with the fact that the break-through force is higher at high loading rates and so should be the elastic deformation of the monolayer. One should also notice that the deformation of the monolayer at the break-through and at a given loading rate is independent of the monolayer polymerization state. Using these data, one can plot the average break-through force with respect to the average tip jump height. Data measured before and after polymerization on the same monolayer are shown in Figure 5. Both the Young's modulus and the monolayer thickness can be determined by fitting the data with eq 1. The monolayer thickness corresponds to the value of the tip jump height for which a break-through force of zero would be obtained, i.e., when there is no indentation of the tip in the monolayer. For both types of monolayers, we find a value of 3.3 ± 0.2 nm in good agreement with expected values of 3.0 ± 0.3 nm as previously determined from AFM imaging in solution. The values of the Young's modulus for each type of monolayers are reported in Table 1.

Table 1. Average values of the Young modulus, k_0, and Gibbs energy deduced from three different sets of measurements before and after polymerization

experiment	E (MPa)	k_0 (s^{-1})	ΔG^0 (k_BT)
before polymerization	2.0 ± 2.5	1068 ± 353	2.6 ± 0.4
after polymerization	229 ± 109	9.2 ± 1.6	7.3 ± 0.2

Before polymerization, a value of the Young's modulus of 2.0 ± 2.5 MPa is obtained. This value perfectly falls into the range of young moduli that were previously reported for supported lipid bilayers of other type of lipids (20 kPa to 20 MPa).[13,15,20,37,38] After the polymerization, a large increase of the young's modulus is obtained with a value of 229 ± 109 MPa. The large error bars which are reported here for both types of monolayers must arise from some variability in the quality of the monolayers. We have to keep in mind however that the apparent Young's moduli determined here are certainly overestimated by the presence of the hard substrate below the monolayers. It was shown before that to avoid this type of substrate effect the indentation should not be larger than 10% of the monolayer thickness.[13] In our measurements, it ranges from 11% to 38%. Several models have been proposed to correct this effect using modified Young's moduli that would integrate the substrate effect but these do not apply to such thin layers.[38−46] Nevertheless, since the deformation of the monolayer is similar for the two types of surfaces, the same substrate effect must apply, and the data can be compared. The results clearly evidence an effect of the polymerization on the elastic properties of the lipid monolayer with a large increase of the Young's modulus. After polymerization, this value is comparable to that of low density polyethylene used to make plastic bags (~200 MPa).

Determination of the Intrinsic Gibbs Activation Energy for the Formation of a Hole. The intrinsic Gibbs activation energy, ΔG^0 ($\Delta G(t = 0)$), of our system corresponds to the energy required for the formation of a hole which is large enough for the tip to penetrate the monolayer when no force is exerted by the tip, i.e., at time $t = 0$ when the tip is just in contact with the monolayer.[28] The rate at which this hole is formed spontaneously, k_0, and ΔG^0 are related as

$$k_0 = k'_0 e^{-\Delta G^0/k_BT} \quad (2)$$

where k_0' is the total number of penetration attempt per seconds and corresponds to the resonant frequency of the tip (~14 kHz).

Franz et al.[28] have shown that k_0 can be deduced from the fit of the experimental data in Figure 4 as

dx.doi.org/10.1021/jp302306r | J. Phys. Chem. B 2012, 116, 7190−7195

$$k_0 = \frac{K}{b \log(e)} 10^{-a/b} \quad (3)$$

with a and b being the two fitting parameters and K being the spring constant of the cantilever. The values of k_0 obtained for the two types of monolayers are reported in Table 1 together with the resulting intrinsic Gibbs activation energies determined using eq 2. Values of k_0 of typically 1050 s^{-1} obtained before the polymerization are reduced by a factor of 100 after polymerization therefore indicating a better stability of the polymerized lipid monolayer. For both types of monolayers, the intrinsic Gibbs activation energies derived from eq 2 are 2.6 ± 0.4 k_BT (6.4 ± 0.9 kJ/mol) and 7.3 ± 0.2 k_BT (18 ± 0.4 kJ/mol) respectively. Considering that the formation of a hole is due to the diffusion of the lipids under the tip, it is reasonable to compare these Gibbs energies to the energy of diffusion of lipids in layers. For DPPC bilayers, energies ranging from 20 to 50 kJ/mol have been reported in the literature using fluorescence technique[47,48] and ^{1}H NMR.[49] Although a little bit smaller, the values of the Gibbs energies that we report here are reasonable considering that our measurements were realized on monolayers instead of bilayers. Indeed, the amount of lipids to displace to allow the tip penetration is twice as high in a bilayer. Similarly, in such force measurement experiments, the size and the shape of the tip will have an effect on the outcoming values. Nevertheless, the effect of the polymerization on the Gibbs energy of the tip/monolayer system is demonstrated with a variation by a factor of ∼3.

CONCLUSIONS

In this work, we have investigated the effect of polymerization on the nanomechanical properties of supported lipid monolayers. We have demonstrated that as for bilayers, the force required to rupture monolayers has a logarithmic dependence on the tip loading rate. We have shown that this range of forces varies drastically with the polymerization state of the monolayer with a large increase by a factor of ∼10 after polymerization. Similarly both the Young's modulus determined for each type of monolayer and the intrinsic Gibbs activation energies of the tip/monolayer system required to initiate the rupture of the monolayer evidence an improvement of the nanomechanical stability of the monolayer after polymerization. The utilization of lipid monolayers or bilayers in industrial processes has been so far limited by their inherent instability in air and mechanical fragility. We believe these layers with improved stability will open a whole range of possibilities in applications that require the use of ultrathin layers. Our interest concerns the development of high sensitivity field effect transistors based biosensors that use a lipid monolayer as gate dielectric. More generally these layers could be used to functionalize flexible materials used in bioelectronics applications for example.

AUTHOR INFORMATION

Corresponding Author

*E-mail: charrier@cinam.univ-mrs.fr. Phone: +33 (0)6 62 92 28 35.

Notes

The authors declare no competing financial interest.

ACKNOWLEDGMENTS

We acknowledge the financial support of the PACA regional council in France (Contract No. DEB 10-1174) as well as Pierre-Henri Puech, from the Adhesion and Inflammation Laboratory in Marseille, for fruitful scientific discussions.

REFERENCES

(1) Kovalev, A.; Shulha, H.; Lemieux, M.; Myshkin, N.; Tsukruk, V. V. *J. Mater. Res.* **2004**, *19*, 716.
(2) VanLandingham, M. R.; Villarrubia, J. S.; Gurthie, W. F.; Meyers, G. F. *Macromol. Symp.* **2001**, *167*, 15.
(3) Shulha, H.; Kovalev, A.; Myshkin, N.; Tsukruk, V. V. *Eur. Polym. J.* **2004**, *40*, 949.
(4) Tsukruk, V. V.; Huang, Z.; Chizhik, S. A.; Gorbunov, V. V. *J. Mater. Sci.* **1998**, *33*, 4905.
(5) Pera, I.; Stark, R.; Kappl, M.; Butt, H. J.; Benfenati, F. *Biophys. J.* **2004**, *87*, 2446.
(6) Künneke, S.; Krüger, D.; Janshoff, A. *Biophys. J.* **2004**, *86*, 1545.
(7) Dufrêne, Y. F.; Lee, G. U. *Biochim. Biophys. Acta* **2000**, *1509*, 14.
(8) Park, J.-W. *Col. Surf. B* **2010**, *75*, 290.
(9) Leonenko, Z.; Finot, E.; Cramb, D. *Biochim. Biophys. Acta* **2006**, *1758*, 487.
(10) Canale, C.; Jacono, M.; Diaspro, A.; Dante, S. *Microsci. Res. Technol.* **2010**, *73*, 965.
(11) Picas, L.; Scheuring, S. *Biophys. J.* **2012**, *102*, L01.
(12) Garcia-Manyes, S.; Sanz, F. *Biochim. Biophys. Acta* **2010**, *1798*, 741.
(13) Ngwa, W.; Chen, K.; Sahgal, A.; Stepanov, E. V.; Luo, W. *Thin Solid Films* **2008**, *516*, 5039.
(14) Dimitriadis, E. K.; Horkay, F.; Maresca, J.; Kachar, B.; Chadwick, R. S. *Biophys. J.* **2002**, *82*, 2798.
(15) Domke, J.; Radmacher, M. *Langmuir* **1998**, *14*, 3320.
(16) Schneider, J.; Dufrêne, Y. F.; Barger, W. R., Jr.; Lee, G. U. *Biophys. J.* **2000**, *79*, 1107.
(17) Alessandrini, A.; Seeger, H. M.; Di Cerbo, A.; Caramaschi, T.; Facci, P. *Soft Matter* **2011**, *7*, 7054.
(18) Goertz, M. P.; Stottrup, B. L.; Houston, J. E.; Zhu, X. Y. *J. Phys. Chem. B* **2009**, *113*, 9335.
(19) Charrier, A.; Thibaudau, F. *Biophys. J.* **2005**, *89*, 1094.
(20) Hianik, T.; Haburcák, M.; Lohner, K.; Prenner, E.; Paltauf, F.; Hermetter, A. *Colloids Surf.* **1998**, *139*, 189.
(21) Sullan, R. M. A.; Li, J. K.; Hao, C.; Walker, G. C.; Zou, S. *Biophys. J.* **2010**, *99*, 507.
(22) Hong, H.; Tamm, L. K. *Proc. Natl. Acad. Sci.* **2004**, *101*, 4065.
(23) Anbazhagan, V.; Schneider, D. *Biochim. Biophys. Acta* **2010**, *1798*, 1899.
(24) Üner, M.; Yener, G. *Int. J. Nanomed.* **2007**, *2*, 289.
(25) Ulrich, A. S. *Biosci. Rep.* **2002**, *22*, 129.
(26) Charrier, A.; Mischki, T.; Lopinski, G. P. *Langmuir* **2010**, *26*, 2538.
(27) Dumas, C.; El Zein, R.; Dallaporta, H.; Charrier, A. *Langmuir* **2011**, *27*, 13643.
(28) Franz, V.; Loi, S.; Müller, H.; Bamberg, E.; Butt, H. J. *Colloids Surf.* **2002**, *23*, 191.
(29) Butt, H. J.; Folker, V. *Phys. Rev. E* **2002**, *66*, 031601.
(30) Loi, S.; Sun, G.; Franz, V.; Butt, H. J. *Phys. Rev. E* **2002**, *66*, 031602.
(31) Trucks, G. W.; Raghavachari, K.; Higashi, G. S.; Chabal, Y. J. *Phys. Rev. Lett.* **1990**, *65*, 504.
(32) Zhao, Y.; Mahajan, N.; Fang, J. *J. Phys. Chem. B* **2006**, *110*, 22060.
(33) Picas, L; Montero, M. T.; Morros, A.; Oncins, G.; Hernandez-Borrel, J. *J. Phys. Chem. B* **2008**, *112*, 10181.
(34) Garcia-Manyes, S.; Redondo-Morata, L.; Oncins, G.; Sanz, F. *J. Am. Chem. Soc.* **2010**, *132*, 12874.
(35) Picas, L.; Suárez-Germà, C.; Montero, M. T.; Hernández-Borrell, J. *J. Phys. Chem. B* **2010**, *114*, 1543.

(36) Oncins, G.; Picas, L.; Hernández-Borrell, J.; Garcia-Manyes, S.; Sanz, F. *Biophys. J.* **2007**, *938*, 2713.
(37) Tvarozek, V.; Hianik, T.; Novonty, I.; Rehacek, V.; Ziegler, W.; Ivanic, R.; Andel, M. *Vaccum* **1998**, *50*, 251.
(38) Hianik, T.; Labajova, A. *Bioelectrochem.* **2002**, *58*, 97.
(39) Laney, D. E.; Garcia, R. A.; Parsons, S. M.; Hansma, H. G. *Biophys. J.* **1997**, *72*, 806.
(40) Menčík, J.; Munz, D.; Quandt, E.; Weppelmann, E. R.; Swain, M. V. *J. Mater. Res.* **1997**, *12*, 2475.
(41) Gao, H.; Chiu, C. H.; Lee, J. *Int. J. Sol. Struct.* **1992**, *29*, 2471.
(42) King, R. B. *Int. J. Sol. Struct.* **1987**, *23*, 1657.
(43) Saha, R.; Nix, W. D. *Mater. Sci. Eng., A* **2001**, *319*−*321*, 898.
(44) Tricoteaux, A.; Duarte, G.; Chicot, D.; Le Bourhis, E.; Bemporad, E.; Lesage. *J. Mech. Mater.* **2010**, *42*, 166.
(45) Saha, R.; Nix, W. D. *Acta Mater.* **2002**, *50*, 23.
(46) Chizhik, S. A.; Gorbunov, V. V.; Luzinov, I.; Fuchigami, N.; Tsukruk, V. V. *Macromol. Symp.* **2001**, *167*, 167.
(47) Vaz, W.; Clegg, R.; Hallmann, D. *Biochemistry* **1985**, *24*, 781.
(48) Karakatsanis, P.; Bayerl, T. M. *Phys. Rev. E* **1996**, *54*, 1785.
(49) Galla, H.-J.; Hartmann, W.; Theilen, U.; Sackmann, E. J. *Membr. Biol.* **1979**, *48*, 215.